XRMON-GF EXPERIMENTAL SET-UP DEVOTED TO X-RAY RADIOGRAPHIC OBSERVATION OF DIRECTIONAL SOLIDIFICATION UNDER MICROGRAVITY ON MASER12 SOUNDING ROCKET MISSION

H. Nguyen-Thi[1,2], A.Bogno[1,2], G. Reinhart[1,2], B. Billia[1,2], R.H. Mathiesen[3], G. Zimmermann[4], Y. Houltz[5], K. Löth[5], D. Voss[6], A. Verga[6], F. de Pascale[6]

[1]Aix Marseille Université & [2]CNRS, IM2NP UMR 6242
Campus Saint-Jérôme, Case 142, 13397 Marseille Cedex 20, France, henri.nguyen-thi@im2np.fr
[3]Dept. of physics, NTNU, N-7491 Trondheim, Norway, ragmat@phys.ntnu.no
[4]ACCESS e.V., Intzestrasse 5, 52072 Aachen, Germany, g.zimmermann@access.rwth-aachen.de
[5]Swedish Space Corporation, P.O. Box 4207, SE-171 04 Solna, Sweden, ylva.houltz@ssc.se
[6]European Space Research & Technology Centre, Keplerlaan 1 Postbus 299, 2200 AG Noordwijk, the Netherlands, daniela.Voss@esa.int

ABSTRACT

Structural material properties are related to their solidification microstructures which can be columnar (oriented properties) or equiaxed (isotropic properties). The control of the columnar-to-equiaxed transition is thus crucial in engineering and is still a debated subject. On Earth, natural convection in the melt is the major source of various disturbing effects. Solidification under microgravity is an efficient way to eliminate buoyancy and convection to provide benchmark data for the validation of models and numerical simulations.

The main objective of the ESA - MAP research project entitled XRMON is to conceive and perform *in situ* X-ray radiography experiments on metallurgical processes in microgravity environment. XRMON has been selected to be flown on the MASER 12 sounding rocket mission, scheduled in autumn 2011. This paper reports on the breadboard tests carried out with a dedicated novel experimental set-up developed by SSC (Swedish Space Corporation). Preliminary results confirm the great interest to perform *in situ* characterization to analyse dynamical phenomena during solidification processes.

1. Scientific background

1.1. Columnar to Equiaxed Transition (CET)

Solidification of metallic alloys is characterized by a wide variety of microstructures. The most common structure is the dendrite, which can be either columnar or equiaxed. The grain structure is called columnar if the growth is preferentially oriented in a direction close to the heat flux, whereas equiaxed grains are growing in all space directions, leading to a material with more isotropic macroscopic mechanical properties and a more homogeneous composition field than with columnar microstructure. Depending on the application, one type of grain structure is preferred and thus favoured, e.g. equiaxed grains in car engines and columnar grains in turbine blades. As a consequence, it is critical for industrial applications to understand the physical mechanisms, which control the transition from columnar to equiaxed dendrites (CET). During columnar solidification, CET occurs when equiaxed grains can grow from nuclei present in the undercooled melt ahead of the dendrite tips [1], as shown in Fig.1a. Thus, the first issue in CET is the origin of the nuclei ahead of the columnar front and how to control their density. For industrial application, equiaxed growth can be provoked and controlled by adding refiners (particles acting as preferred nucleation sites for new grains) in the melt. In that case, nuclei result from the heterogeneous nucleation on refining particles [2]. The second mechanism is the detachment of dendrite arms in the mushy zone, which can then be carried into the undercooled liquid by fluid flow. This mechanism is presently considered to be the phenomenon behind the appearance of equiaxed core regions in castings of non-refined alloys [3]. CET occurs in a subsequent stage, if the number and size of equiaxed grains ahead of the columnar front become sufficient, i.e. the columnar growth is stopped and an equiaxed microstructure then prevails [4-6].

In Fig.1b, we present a longitudinal section of an experiment performed in an Al – 3.5 wt% Ni alloy, at a constant thermal gradient of 20 K/cm, with a pulling rate jump from 2 µm/s to 20 µm/s. CET clearly occurred in the grain structure under these test conditions, due to the fact that at a higher pulling rate, the constitutional undercooling on top of the columnar dendrites increases. This enables the activation of some of the refining particles ahead of the columnar front, i.e. the growth of equiaxed grains initiated on these particles. It is worth noting that some equiaxed grains are observed to be embedded in the columnar dendrites.

Proc. '20th ESA Symposium on European Rocket and Balloon Programmes and Related Research'
Hyère, France, 22–26 May 2011 (ESA SP-700, October 2011)

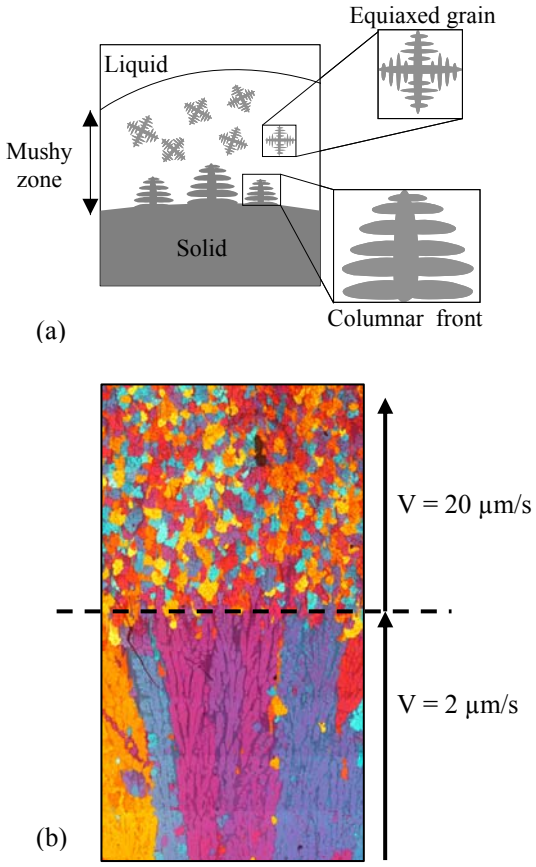

Figure 1. (a) Columnar-to-Equiaxed Transition (CET) during directional solidification
(b) CET in a refined Al - 3.5 wt.%Ni alloy solidified at G = 20 K/cm with a pulling rate jump from V = 2 µm/s to V = 20 µm/s. Image width = 6 mm

1.2. Microgravity relevance

During the solidification of metallic alloys, it is well known that the fluid flow induced by thermal-solutal buoyancy affects dendrite growth and the resulting grain structure. On Earth (1g), natural convection in the melt is well known to be the major source of various disturbing effects which can significantly modify or hinder important physical mechanisms [7,8]. For the CET, fluid flow can be the cause of dendrite arms remelting, leading to dendrite fragmentation [9,10]. The dendrite fragments can be then transported ahead of the columnar front and promote the formation of equiaxed grains. Elsewhere, just after the formation of equiaxed grains ahead of the columnar front, either sedimentation or floating of the equiaxed grains are commonly observed on earth [6,11,12]. For upward solidification, when sedimentation occurs, CET is expected to occur earlier as grains fall and interact strongly with columnar front [13]. On contrary, when equiaxed grains are carried out far away in the liquid phase, CET may be never achieved.

Solidification under microgravity (µg) is thus an efficient way to eliminate all these disturbing effects to provide benchmark data in purely diffusive conditions for the validation of models and numerical simulations. In addition, a comparative study of solidification experiments at 1g and µg can also enlighten the effects of gravity [14,15].

2. XRMON PROJECT

The interaction of equiaxed grains with one another and with the columnar front is essentially dynamical. Consequently, it is of major interest to be able to investigate the time evolution of dynamical selection of the interface pattern during the solidification of metallic alloys. *In situ* and real-time imaging of the metallic alloy solidification can be achieved by applying synchrotron X-ray techniques, in particular X-ray radiography [16,17]. X-ray radiography is particularly well suited for *in situ* studies, since it does not require specific sample environmental conditions and is non-destructive to most materials. In this technique, the contrast in the recorded image is due to local changes in the amplitude and/or phase of the X-ray beam transmitted through the sample. A (monochromatic) X-ray beam illuminates the sample and a 2D-detector (photographic film or CCD camera) is placed close to the sample to record the transmitted beam. In alloy systems, contrast mainly results from segregation of the chemical species and is generally weak and therefore difficult to reveal with conventional X-ray sources.

Recent developments of more powerful synchrotron X-ray sources have lead to vast improvements in the performance of X-ray-based techniques. This is illustrated by a continuous increase in the impact of synchrotron experiments in many areas of materials research, and has also contributed positively to the performance of analysis techniques based on radiation from conventional sources. These recent advances have also revitalized the use of *in situ* X-ray imaging methods in the field of solidification science, where it has now become possible to study alloy growth processes with spatio-temporal resolutions at relevant scales to microstructure formation.

XRMON (*In situ* X-ray monitoring of advanced metallurgical processes under micro gravity and terrestrial conditions) is a Microgravity Application Promotion (MAP) programme of the European Space Agency (ESA). The main scientific objectives of XRMON are:

- Developing *in situ* X-ray radiography as one of the most important experimental techniques in solidification science by demonstrating its potential for high-value input in a broad range of major research subjects.
- Providing experimental results of high relevance to a series of running MAPs and other science projects in the field.
- Demonstrating the new opportunities it offers through a few selected case studies.
- Providing and comparing data from ground-based and microgravity experimentation. For this purpose, three XRMON experiments have been selected to be performed in microgravity. The first one was devoted to the study of metallic foams on both parabolic flight (46th ESA campaign, 2007) and sounding rocket (MASER11, 2008). The second selected experiment deals with the CET and is planned to flight on MASER12 (autumn 2011). The last experiment is dedicated to the measurement of diffusion in melts and is in the preparation phase at the moment (MAXUS9, 2013).

3. EXPERIMENTS

3.1. XRMON - Gradient Furnace set-up

To provide an opportunity to use X-ray diagnostics in microgravity solidification experiments, ESA initiated a hardware development project. The objective was the "Design, manufacturing and testing of a fully functional X-ray diagnostics breadboard suitable for the *in situ* investigation of directional solidification in alloy melts up to 1100K". The conceptual design of the breadboard setup is given in Fig.2. It consists of a gradient furnace system for solidification of AlCu-based alloys and an attached high-resolution X-ray diagnostic system.

For directional solidification experiments a Bridgman type furnace was designed and manufactured. The most challenging tasks for the development came from the combination of a sophisticated gradient furnace for rather high temperatures and the required spatial resolution of the X-ray diagnostics. This implied that the furnace had to be placed so that the distance between source and sample was about 5 mm. This short distance required special thermal insulation to avoid heat leakage from the sample to the cooled target. In addition such a thermal insulation had to be transparent to X-rays as much as possible to guarantee maximum intensity.

The metallic samples had a sheet-like geometry with a length of 50mm, a width of 5mm and a constant thickness of less than 0.2mm along the sample. Each sample was first mechanically polished down to the desired thickness (with a surface rugosity of 1µm), and then spray coated with boron nitride (BN). Then it was sandwiched between two rectangular glass plates, welded together. The BN coating was required because of its combination of properties: *i)* it prevents chemical reaction between the Al-Cu sample and the glass plates and *ii)* it is transparent to X-rays in the range of energy of our interest.

To investigate the dynamics of solidification processes, the field of view for the X-ray diagnostics was about 5 x 5 mm² with a spatial resolution of 3-5 µm and a temporal resolution of 2-3 Hz. The X-ray source was based on a microfocus transmission target in molybdenum using polychromatic radiation with a peak at 17.5 keV. More details are given in another paper (A-042) at this conference.

(a)

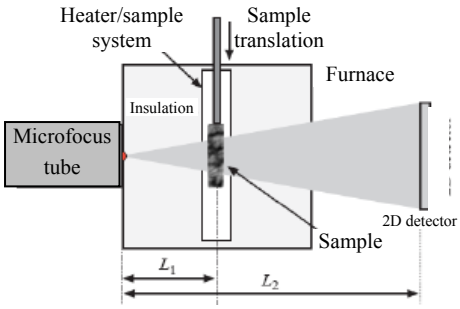

(b)

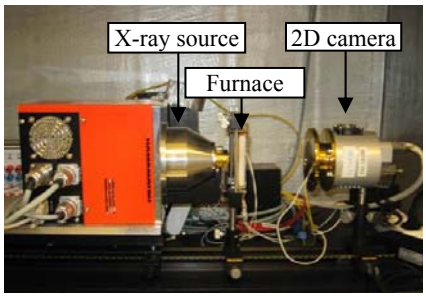

(c)

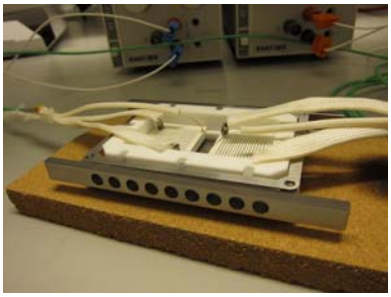

Figure 2. (a) Conceptual design of the breadboard setup, (b) picture of the breadboard setup showing the X-ray source (left), the furnace (very close to the microfocus source) and the detector (right), (c) picture of the furnace (prototype 2)

3.2. Breadboard experiments

Two campaigns of breadboard tests were carried out in Solna (Sweden) at SSC (Swedish Space Corporation). The main objectives of the tests were:

- Testing and validating a furnace design compatible with the scientific requirements (e.g. temperature gradient) and technical constraints (as pointed out in section 3.1.).
- Choosing a crucible design (material, dimension) compatible with X-ray radiography requirements.
- Deciding on sample composition and dimensions.
- Testing flight - like control electronics.
- Demonstrating the feasibility of a solidification experiment with this experimental set-up.
- Providing ground-based reference experiments, showing the strong effects of gravity.

In order to achieve these goals, several series of solidification experiments were carried out by varying the Al-Cu solute compositions C_0 and the temperature gradients G. For each experiment, the sample was first melted above the liquidus temperature and the melting was monitored by X-ray radiography to check the isotherm planarity. In a second step, a stabilisation phase of at least two hours was applied to ensure an homogenised solute distribution along the sample. Solidification was then induced by applying the *power-down* method, with displacement of neither the sample nor the furnace. In this method, the temperatures of the hot and cold zones of the furnace were first adjusted to achieve the desired temperature gradient. Then, solidification was triggered by applying either a cooling rate $R_H \neq 0$ only on the hot zone of the furnace while maintaining the cold zone temperature constant ($R_C = 0$) or the same cooling rate ($R_H = R_C$) on both heater elements. Regardless of the solidification procedure, growth occurred in unsteady thermal conditions during the whole experiment.

Image processing was applied to improve the quality of the radiographs. It consisted in dividing the raw image of the sample taken at time t (Fig.3a), during solidification, by a reference image recorded at initial time t_0 (Fig.3b), chosen just before cooling down starts when the sample was mostly liquid and homogeneous with a constant initial solute concentration C_0 [18]. The result was an enhanced contrast and a defect free image (Fig.3c), where Al-enriched dendrites appear in white, surrounded by a dark Cu-enriched liquid. In practice, this image processing method is easier when the sample is fixed in the field of view, which is the case when directional solidification is triggered by using the *power-down* method.

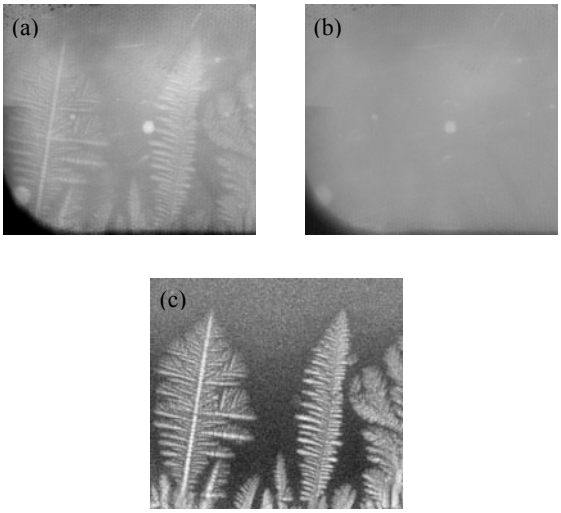

Figure 3. Columnar dendritic solidification of Al-10wt% Cu (R_H=12K/min; R_C=0; G=40 K/cm). Image width= 3.8 mm
(a) Raw image at time $t = t_0 + 80$s during the solidification; (b) Raw image at reference time t_0 and (c) Processed image obtained by dividing Fig.3a by Fig.3b. Al-rich dendrites appears in light whereas Cu-enriched liquid appears in dark.

4. BREADBOARD TEST RESULTS

4.1. Initial transient during directional solidification of Al - 10 wt% Cu alloy

Fig.4 shows a sequence of six images taken during the initial solidification transient of an Al - 10 wt% Cu alloy for a temperature gradient of 43 K/cm and a cooling rate of the hot heater element R_H = 6 K/min (with R_C = 0K/min). This figure illustrates the great advantage of using X-ray radiography for *in situ* investigation of directional solidification of metallic alloys. This sequence of images shows the time evolution of the interface pattern, from the breakdown of the planar interface to the subsequent developments of the microstructure. The vertical black strip visible on the left of all the figures is an artefact due to the image processing.

For this experiment, the solidification microstructure was photographed every 2 seconds with an exposure time of 2 seconds. In Fig.4a ($t = t_0 + 150$s, with t_0 the reference time, just before the beginning of the solidification) the first disturbances are visible along the whole interface, following the planar front breakdown induced by the Mullins–Sekerka instability [19]. It is worth noting that the macroscopic planarity of the interface is quite excellent, which was one of the most

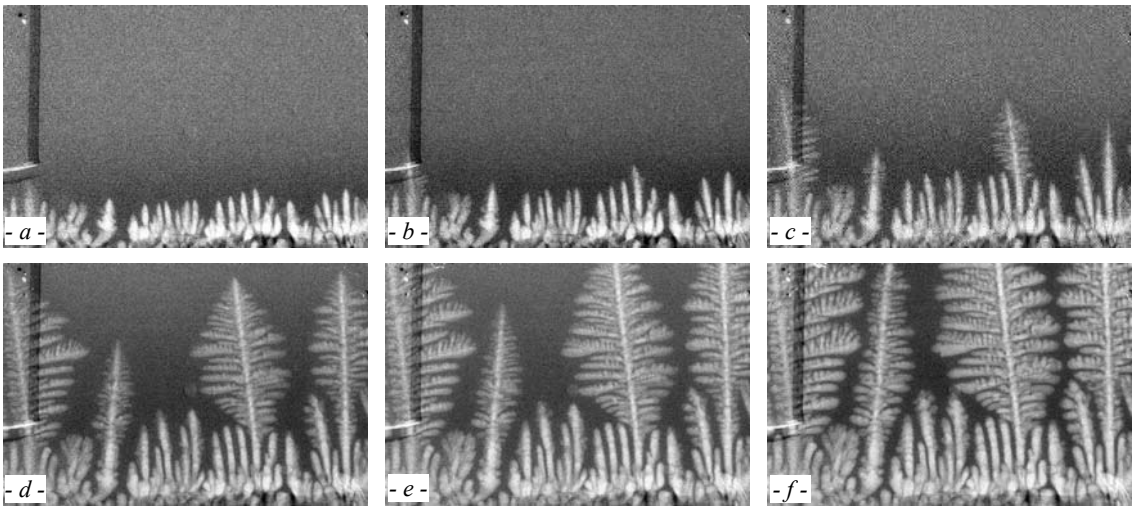

Figure 4. Sequence of six radiographies showing the formation of a columnar structure of Al-10wt% Cu (R_H = 6K/min; R_C = 0; G ≈ 43 K/cm) (a) t=t_0+150s; (b) t=t_0+170s; (c) t=t_0+200s; (d) t= t_0+260s; (e) t=t_0+300s; (f) t=t_0+400s. t_0 is the reference time, just before the beginning of the solidification. Image width=4.5 mm.

important scientific requirements and confirms the good thermal behaviour of the furnace. In addition, one can already see in Fig.4a that side branches begin to grow on most of the perturbations, which indicates the inception of the formation of dendrites. At this stage, it is possible to determine an average wavelength λ_i for the microstructure, $\lambda_i \approx 180$ µm. Further development of the pattern occurs with a progressive increase of the amplitude of the disturbances (Fig. 4b, t = t_0 + 170s), while the liquid ahead of the columnar front becomes darker and darker, due to the solute rejection during the liquid-solid transformation.

In the subsequent stages, both the amplitude and lateral size of dendrite increase concomitantly, with solute screening causing a strong decrease of the growth of the neighbouring dendrites. In our experiments, a steady state was never achieved for several reasons: *(i)* the power-down technique used to trigger the solidification, *(ii)* the low value of the partition coefficient ($k \approx 0.14$) which implies a long transient regime, and *(iii)* the short sample length (about 50 mm). Nevertheless, the general shape of the microstructure does not change drastically in the latest stages of solidification and is mainly composed of several dendrites protruding markedly into the liquid phase with an average final primary spacing $\lambda_f \approx 1{,}260$µm (Fig.4f).

4.2. Fragmentation phenomenon during solidification of Al – 20 wt% Cu alloy

One mechanism for the formation of equiaxed grains is the dendrite fragmentation [1], which is believed to be at the origin of the central equiaxed core region in casting processes.

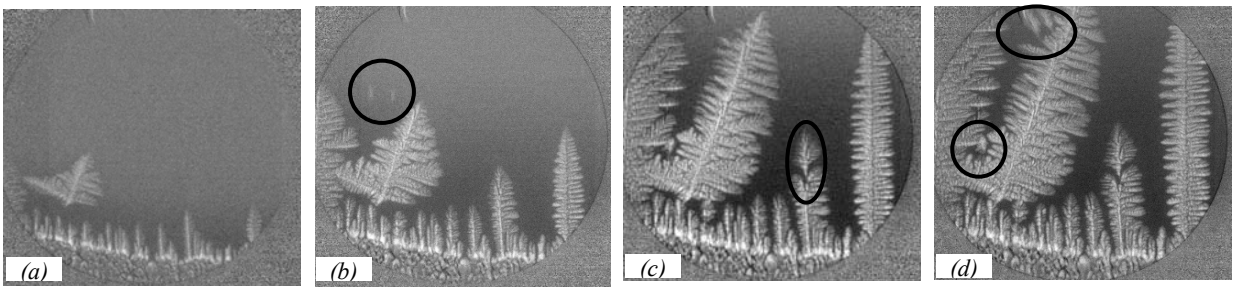

Figure 5. Sequence of 4 radiographies during columnar growth of Al-20wt% Cu showing several dendrite fragmentations (R_H = 20K/min; R_C=0; G = 400 K/cm) (a) t=t_0+50s; (b) t=t_0+100s; (c) t=t_0+150s; (d) t=t_0+168s. t_0 is the reference time, just before the beginning of the solidification. Image width=5 mm.

Fragmentation occurs when dendrite branches are detached from the main primary trunks. If these fragments are transported ahead of the columnar front by buoyancy forces or convection, they can continue to grow and then form equiaxed grains that can stop the advancing columnar front. Fragmentation is favoured by the dendrite ripening process but also by the initiation of local remelting due to the local pile-up of solute within the partially solid-liquid sample region usually called the "mushy zone" [10,20,21].

Forced convection like electromagnetic stirring, axial vibrations or the accelerated crucible rotation technique can also create conditions for fragmentation. The use of a forced field is accompanied by enhancement of stirring that can also help to transport fragments to places where they can grow and provoke CET.

Fragmentation is an essential feature of the CET; however, the details of the fragmentation phenomenon are insufficiently understood and controlled. Thus, one of the main objectives is to confirm the predominance of the fragmentation phenomenon in CET in non-refined alloys and also to improve the characterisation and understanding of its mechanism, in particular the role of gravity at each step of CET. To achieve this goal, an efficient approach is to perform a comparison between solidification experiments carried out at 1g and in μg, in both cases with *in situ* characterization by means of X-ray radiography. Several experiments were performed on a single non-refined Al – 20 wt% Cu sample, for various high temperature gradients (200 - 400 K/cm) and cooling rates (R_H= 1 – 20 K/min, R_C = 0 K/min). For the experiment presented in Fig.5, the high nominal solute concentration lead to a higher contrast than in previous experiment with an Al – 10 wt% Cu. Therefore, the exposure time was reduced to one second, and the evolution of the solidification microstructure was recorded every second. In Fig.5a one can see the gradual establishment of columnar growth, as described in the previous section. In this experiment, an equiaxed grain had nucleated ahead of the columnar front, on a small heterogeneity. This grain remained fixed and simply continued to grow in interaction with the columnar front.

In Fig.5b and Fig.5d, the black circles pinpoint the presence of several dendrite fragments. For Al – 20 wt% Cu, the solid (mainly composed of aluminium) being much lighter than the surrounding liquid (Cu - enriched), dendrite fragmentation was promoted by buoyancy forces acting on secondary dendrite arms.

After the fragmentation, the dendrite pieces were immediately carried away to the upper part of the sample. In this experiment, fragmentation occurred continuously during the growth process. Radiographs made it possible to have a rough estimation of the fragments velocity, typically about 60 μm/s in this experiment. It is worth noticing that these dendrite fragments could not promote CET, because they were carried up far into the liquid where they were re-melted. Furthermore, the fact that all Al-enriched dendrite fragments were transported by buoyancy forces into the upper part of the sample was at the origin of a strong segregation along the sample as the solidification front advanced.

In Fig.5c, the fragmentation of a dendrite primary trunk can be noticed, indicated by a black ellipse. Its size being large compared to the sample thickness, the primary trunk fragment could not move far into the liquid phase. This phenomenon was rarely observed compared to the secondary dendrite arm fragmentation, certainly because of the difference in diameter between primary trunk and secondary arms. It has recently been observed by using combined radiography and topography the rotation of some tenth of degrees around the growth axis of the entire primary trunk during the growth process [22]. This rotation has been interpreted as a consequence of a torque induced by shear stress that builds up with the growth [23]. This suggests that stress accumulates there to finally provoke the trunk to crack. In our experiments, it was also observed that this phenomenon occurred mainly for a specific crystallographic dendrite direction <110>, which suggests an effect of dendrite morphology.

4.3. Visualisation of convection rolls above the solid-liquid interface during melting process

Fig.6 displays a sequence of 3 radiographs taken just after the stabilization phase, during a short melting experiment. In Fig.6a one can distinguish the unmelted part of the sample at the bottom (solid), the molten part at the top and a very thin Al-rich solidified layer in between them. In Fig.6b this layer has melted and has become dark due to the image processing. The white layer just above the black layer is the liquid phase that is Al-enriched, due to the rejection of aluminium during the melting process. The solute-rich melt is less dense compared to the initial liquid composition, so that density stratification is unstable and provokes solutal convection in the form of convective rolls ahead of the melting front. In Fig.6c, the four convective rolls are pinpointed by white arrows. These last series of pictures thus demonstrate the high capabilities of the X-ray device developed in the frame of the XRMON project to provide a real-time diagnostic technique during solidification or melting of Al- based alloys.

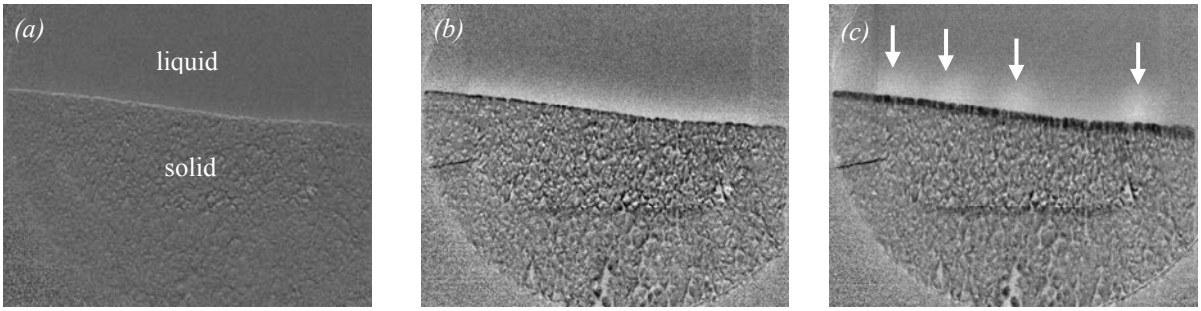

Figure 6. Sequence of three radiographies during the melting of an Al-20wt% Cu showing 4 convective rolls of Al-rich liquid (estimated heating rate=7.5K/min; G =145K/cm) (a) $t=t_0=20s$; (b) $t=t_0+8s$; (c) $t=t_0+16s$; t_0 is the time when melting started. Image width=5 mm.

5. CONCLUSIONS

This paper reports on a selection of preliminary results obtained during two series of breadboard tests carried out with a dedicated novel experimental set-up developed by SSC in the frame of the ESA-MAP XRMON. These results validate the experimental set-up in terms of thermal behaviour and X-ray imaging, which were very challenging issues at the beginning of the project. From a scientific point of view, these breadboard results show the great impact of gravity and convection on the dynamics of the solidification front.
The next step of the project is *i)* the validation of the flight model of the set-up and *ii)* the precise definition of a CET experiment, which is a key issue owing to the short duration of the microgravity period (about 6 minutes) during a MASER sounding rocket mission. The ultimate goal will be to carry out the Columnar – to – equiaxed Transition experiment during MASER12 mission in autumn 2011.

6. ACKNOWLEDMENTS

This research work is supported by the XRMON project (AO-2004-046) of the MAP program of the European Space Agency (ESA) and by the French National Space Agency (CNES).

7. REFERENCES

1. Spittle, J. A. Columnar to equiaxed grain transition in as solidified alloys; *International Materials Reviews* **2006**, *51*, 247.
2. Greer, A. L.; Bunn, A. M.; Tronche, A.; Evans, P. V.; Bristow, D. J. Modelling of inoculation of metallic melts: application to grain refinement of aluminium by Al-Ti-B; *Acta Materialia* **2000**, *48*, 2823.
3. Gandin, C. A. From constrained to unconstrained growth during directional solidification; *Acta materiala* **2000**, *48*, 2483.
4. Hunt, J. D. Steady State Columnar and Equiaxed Growth of Dendrites and Eutectic; *Materials Science and Engineering* **1984**, *65*, 75.
5. Martorano, M. A.; Beckermann, C.; Gandin, C.-A. A solutal Interaction Mechanism for the Columnar-to-Equiaxed Transition in Alloy Solidification; *Metallurgical and Materials Transactions A* **2003**, *34A*, 1657.
6. Reinhart, G.; Nguyen-Thi, H.; Mangelinck-Noël, N.; Schenk, T.; Billia, B.; Gastaldi, J.; Härtwig, J.; Baruchel, J. in-situ observation of transition from columnar to equiaxed growth in al-3.5 wt% ni alloys by synchrotron radiography; *Modeling of Casting, Welding and Advanced Solidification Processes* **2006**, *XI*, 359.
7. Davis, S. H. Hydrodynamics Interactions in Directional Solidification; *J. Fluid Mech.* **1990**, *212*, 241.
8. Jamgotchian, H.; Nguyen Thi, H.; Bergeon, N.; Billia, B. Double-diffusive convective modes and induced microstructure localisation during solidification of binary alloys; *International Journal of Thermal Sciences* **2004**, *43*, 769.
9. Hellawell, A.; Liu, S.; Lu, S. Z. Dendrite fragmentation and the effects of fluid flow in castings; *JOM-J. Miner. Met. Mater. Soc.* **1997**, *49*, 18.
10. Ruvalcaba, D.; Mathiesen, R. H.; Eskin, D. G.; Arnberg, L.; Katgerman, L. In situ observations of dendritic fragmentation due to local solute-enrichment during directional solidification of an aluminum alloy; *Acta Materialia* **2007**, *55*, 4287.
11. Mirihanage, W. U.; Browne, D. J. Sedimentation speed of a free dendrite growing in an undercooled melt; *Computational Materials Science* **2010**, *50*, 260.

12. Badillo, A.; Beckermann, C. In *5th Decennial International Conference on Solidification processing*; Jones, H., Ed.; University of Sheffield, UK: Sheffield, UK, 2007, p 316.
13. Nguyen Thi, H.; Reinhart, G.; Mangelinck-Noël, N.; Jung, H.; Billia, B.; Schenk, T.; Gastaldi, J.; Härtwig, J.; Baruchel, J. In-Situ and Real-Time Investigation of Columnar to Equiaxed Transition in Metallic Alloy; *Metall. Mater. Trans. A* **2007**, *38-7*, 1458.
14. Nguyen Thi, H.; Dabo, Y.; Drevet, B.; Dupouy, M. D.; Camel, D.; Billia, B.; Hunt, J. D.; Chilton, A. Directional Solidification of Al-1.5wt% Ni alloys under diffusion transport in space and fluid flow localisation on Earth; *J. of Crystal Growth* **2005**, *281*, 654.
15. Drevet, B.; Nguyen Thi, H.; Camel, D.; Billia, B.; Dupouy, M. D. Solidification of Aluminum-Lithium Alloys near the Cell/Dendrite Transition - Influence of Solutal Convection; *J. Crystal Growth* **2000**, *218*, 419.
16. Mathiesen, R. H.; Arnberg, L.; Ramsokar, K.; Weitkamp, T.; Rau, C.; Snigirev, A. Time-resolved X-Ray Imaging of Dendritic Growth in Binary Alloys; *Phys. Rev. Lett.* **1999**, *83*, 5062.
17. Schenk, T.; Nguyen Thi, H.; Gastaldi, J.; Reinhart, G.; Cristiglio, V.; Mangelinck-Noël, N.; Klein, H.; Härtwig, J.; Grushko, B.; Billia, B.; Baruchel, J. Application of synchrotron X-ray imaging to the study of directional solidification of aluminium-based alloys; *Journal of Crystal Growth* **2005**, *275*, 201.
18. Buffet, A.; Nguyen Thi, H.; Bogno, A.; Schenk, T.; Mangelinck-Noël, N.; Reinhart, G.; Bergeon, N.; Billia, B.; Baruchel, J. Measurement of solute profiles by means of synchrotron X-ray radiography during directional solidification of Al - 4 wt% Cu alloys; *Materials Science Forum* **2010**, *649*, 331.
19. Mullins, W. W.; Sekerka, R. F. Stability of a planar interface during solidification of a dilute binary alloy; *J. Appl. Phys.* **1964**, *35*, 444.
20. Jung, H.; Mangelinck-Noel, N.; Nguyen-Thi, H.; Bergeon, N.; Billia, B.; Buffet, A.; Reinhart, G.; Schenk, T.; Baruchel, J. Fragmentation in an Al-7 wt-%Si alloy studied in real time by X-ray synchrotron techniques; *Int. J. Cast. Metals Res.* **2009**, *22*, 208.
21. Mathiesen, R. H.; Arnberg, L.; Bleuet, P.; Somogyi, A. Crystal fragmentation and Columnar - to - Equiaxed Transitions in AlCu Studied by Synchrotron X-Ray Video Microscopy; *Metall. And Mater. Trans. A* **2006**, *37A*, 2515.
22. Reinhart, G.; Buffet, A.; Nguyen-Thi, H.; Billia, B.; Jung, H.; Mangelinck-Noel, N.; Bergeon, N.; Schenk, T.; Hartwig, J.; Baruchel, J. In-Situ and real-time analysis of the formation of strains and microstructure defects during solidification of Al-3.5 wt pct Ni alloys; *Metallurgical and Materials Transactions a-Physical Metallurgy and Materials Science* **2008**, *39A*, 865.
23. Billia, B.; Bergeon, N.; Nguyen Thi, H.; Jamgotchian, H. Cumulative moments and microstructure deformation induced by growth shape in columnar solidification; *Phys. Rev Lett.* **2004**, *93*, 126105.